

# Wideband Microstrip Quasi-Elliptic Function Bandpass Filter with High Out-of-Band Rejection

Bal S. Virdee, Muhammad Riaz, Panchamkumar Shukla, Muhittin Onadim, Karim Ouazzane

London Metropolitan University, Centre for Communications Technology, 166-220 Holloway Road, London, UK.

\*[b.virdee@londonmet.ac.uk](mailto:b.virdee@londonmet.ac.uk)

**Abstract**— Presented in the paper is a novel and compact quasi-elliptic function bandpass filter based on microstrip technology that exhibits a high out-of-band rejection over a very wide frequency range. The design comprises stub loaded half-wavelength resonators that are electromagnetically coupled to resonant structures that are interdigitally coupled to the input and output feed-lines. Perturbation introduced by the presence of the stub causes the resonators to act as a multimode device. In addition, the stub introduces two transmission zeros to significantly improve the filter's passband selectivity and suppress harmonic and spurious modes. This configuration yields a wideband response with low insertion-loss of 0.73 dB, high return-loss < 20 dB, and out-of-band rejection level > 40 dB across 2–4.5 GHz and 5.74–16 GHz. The planar filter structure can be easily manufactured using standard PCB technology.

**Index Terms**— Quasi-elliptic bandpass filter, interdigital coupled feed-line, wideband, wide stopband.

## I. INTRODUCTION

IN recent years, with the rapid develop of wireless microwave systems, different types of bandpass filters are demanded for system implementation including multiband, wideband and ultra-wideband (UWB). Demand for wideband bandpass filters is burgeoning with the increased use of UWB technology. High out-of-band rejection and low insertion-loss are additional requirements sought by such systems to prevent RF electromagnetic interference (EMI) noise affecting other wireless systems; this requirement makes a compact filter design even more challenging. In addition, wide bandwidth requires tight couplings between resonators, implying a large degree of proximity, which makes filter response highly sensitive to fabrication tolerances and reduces power handling capability of such filters. To achieve high selectivity, it is normally necessary to increase the number of resonators which leads to higher passband loss. Alternatively, selectivity can be improved by inserting transmission zeros near the filter's skirts; however, this can complicate the design. Moreover, due to the presence of harmonic modes, the problem of spurious responses arises, which can interfere with other systems.

Stub loaded multiple-mode resonators have been shown to produce wide passband but with narrow stopband [1][2]. It has been demonstrated that extension of the stopband bandwidth

can be achieved by cascading together coplanar waveguide (CPW) structure [3][4], or by employing complementary split ring resonators [5]; the disadvantage of these techniques is a larger circuit footprint. Another technique of designing wideband filters involves broadside coupled microstrip/CPW [6][7]. Although this technique yields a compact circuit design however there is no improvement in the rejection band. Thus, the design of highly compact wideband filters with wide stopband remains a great challenge.

In this paper, a novel compact wideband microstrip filter design is described with the desired electrical characteristics using stub loaded half-wavelength resonators coupled to input and output resonators. The input and output feed-lines are interdigitally coupled to reduce the passband insertion-loss and for the realization of a wide stopband on both sides of the passband with high rejection level. Interdigital coupling is used to reduce the need for tight coupling and to achieve a wide passband. The proposed filter is (i) a simple planar structure which is via-free; and (ii) where the coupling gap dimensions (<100 microns) are not critical, which would otherwise complicate the construction of the filter and therefore exacerbate its manufacturing cost. The proposed filter exhibits excellent wideband characteristics that are normally observed in high temperature superconducting (HTS) bandpass filters [8].

## II. CONFIGURATION OF THE UWB STRUCTURE

The proposed planar microstrip filter is shown in Fig. 1. The input and output feedlines are interdigitally coupled to the filter structure. Length of the interdigital fingers is  $\lambda/4$  in order to enhance the coupling and minimize passband loss performance. Length  $L_{b2}$  controls the out-of-band rejection and to a smaller extend the passband loss of the filter. Coupling gap  $S_4$  between the feed-line resonators and the stub loaded half-wavelength resonator determines the out-of-band rejection and to a lesser extend passband response of the filter. Length  $L_5$  has insignificant effect on the filter's passband response. Length  $L_6$  controls the bandwidth of the filter and to a lesser extend its loss performance. Feedline coupling gap  $S_3$  has significant effect on the out-of-band rejection and passband ripples. Length of  $L_a$  and  $L_{a1}$  are used to control the lower and upper transmission zeros, respectively. The interdigital coupled feed length  $L_{b3}$  controls the out-of-band rejection level. Length  $L_1$  is used to create a notch band that can be shifted to improve the lower out-of-band rejection of the filter. Width  $W_a$  also helps improves the out-of-band rejection level on both sides of the passband. The measured

results given in Section IV confirms the merits of the proposed filter, i.e. low insertion-loss, good passband selectivity, wide stopband, flat group delay, via free, single side implementation, and compact size.

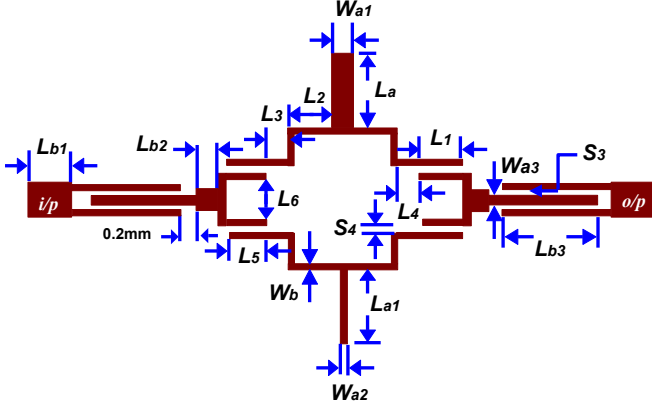


Fig. 1. Microstrip configuration of the proposed wideband filter.

### III. ANALYSIS OF STEP LOADED RESONATOR

The proposed wideband filter is essentially a multimode resonator structure consisting of a stub loaded resonator (SLR) that is implemented by loading a microstrip line with a half-wavelength open stub, as illustrated in Fig. 2, where  $Z_1$ ,  $\theta_1$ , and  $Z_2$ ,  $\theta_2$  represent the characteristic impedance and length of the microstrip-line and open stub, respectively. Since the SLR is symmetrical in structure, odd- and even-mode analysis can be applied to characterize it.

#### A. Odd Mode Analysis

For odd-mode excitation, there is a voltage null in the middle of the SLR, which leads to the equivalent circuit of Fig. 3(a), which is simplified in Fig. 3(b).

$$Z_L = j \frac{Z_2}{2} \cot \theta_2 \quad (1)$$

$\theta_2$  is the electric length of the stub, and  $\theta_1$  is the electric length of the microstrip-line. Then

$$Y_{in\ odd} = -jY_1 \left\{ \frac{Z_1 - \frac{Z_2}{2} \tan \theta_1 \tan \theta_2}{\frac{Z_2}{2} \tan \theta_2 + Z_1 \tan \theta_1} \right\} = 0 \quad (2)$$

At resonance,  $Y_{in\ odd} = 0$ , so

$$\therefore \tan \theta_1 \tan \theta_2 = \frac{2Z_1}{Z_2} = k \quad (3)$$

Resonance condition is determined by  $\theta_1$ ,  $\theta_2$  and impedance ratio  $k$ . The total resonator length and the normalized resonator length are given by

$$\theta_T = \theta_1 + \theta_2 \quad (4)$$

$$\theta_T = \theta_1 + \tan^{-1} \left( \frac{k}{\tan \theta_1} \right) \quad (5)$$

$$L_n = \frac{2}{180^\circ} \left[ \theta_1 + \tan^{-1} \left( \frac{k}{\tan \theta_1} \right) \right] \quad (6)$$

Fig. 4 shows the relationship between  $\theta_T$  and  $L_n$  as a function of  $k$ . The graph shows that  $L_n$  attains maximum value when  $k \geq 1$ , and a minimum value when  $k < 1$ .

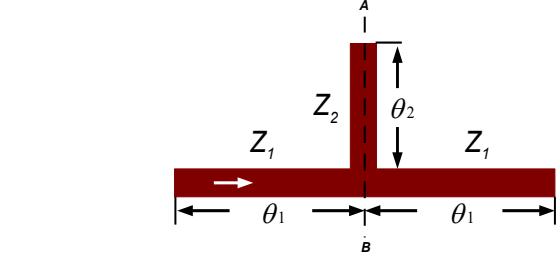


Fig. 2. Structure of the stub-loaded resonator

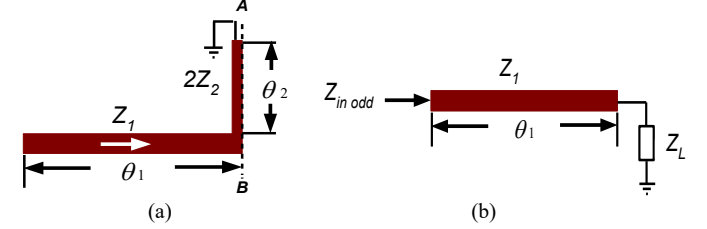


Fig. 3. Equivalent circuit model, (a) odd-mode circuit, and (b) odd-mode circuit model.

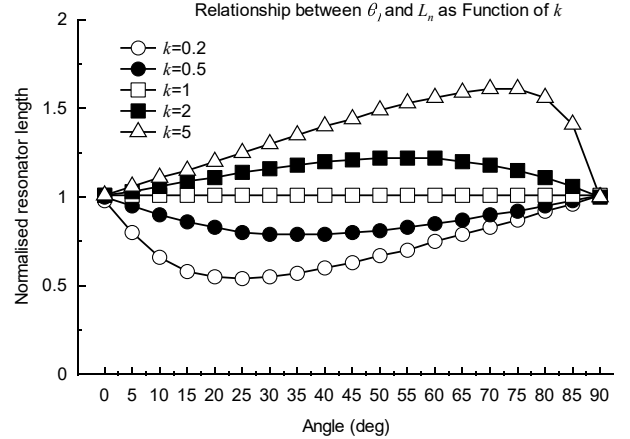


Fig. 4. Normalized resonator length as a function of microstrip-line length (in degrees) for various impedance ratios.

#### Condition for Maximum and Minimum $\theta_T$

The maximum and minimum length  $\theta_T$  can be deduced from Eqn. (3).

$$\theta_T = \theta_1 + \theta_2 \quad (7)$$

When  $0 < k < 1$  and  $0 < \theta_T < \pi/2$

$$\tan \theta_T = \frac{\sqrt{k}}{(1-k)} \left( \frac{\tan \theta_1}{\sqrt{k}} + \frac{\sqrt{k}}{\tan \theta_1} \right) \geq \frac{2\sqrt{k}}{1-k} \quad (8)$$

When  $\frac{\tan \theta_1}{\sqrt{k}} = \frac{\sqrt{k}}{\tan \theta_1}$

$\theta_T$  attains a minimum value of

$$\theta_{T_{min}} = \tan^{-1} \left( \frac{2\sqrt{k}}{1-k} \right) \quad (9)$$

Similarly, if  $k > 1$  and  $\pi/2 < \theta_T < \pi$ , we obtain the following expression

$$\tan\theta_T = -\frac{\sqrt{k}}{1-k} \left( \frac{\tan\theta_1}{\sqrt{k}} + \frac{\sqrt{k}}{\tan\theta_1} \right) \quad (10)$$

As  $0 < \theta_1 < \pi/2$ ,  $\theta_T$  attains a maximum value of

$$\theta_{T_{max}} = \tan^{-1} \left( \frac{2\sqrt{k}}{1-k} \right) \quad (11)$$

when  $\theta_1 = \theta_2 = \tan^{-1}\sqrt{k}$

This analysis reveals that  $\theta_1 = \theta_2$  yields a resonator with maximum and minimum length. When  $\theta_1 = \theta_2 = \theta_o$ , the normalized resonator length is:

$$L_{n_o} = \frac{2\theta_T}{\pi} = \frac{2}{\pi} \tan^{-1}\sqrt{k} \quad (12)$$

The graph in Fig. 5 shows that resonator length can be reduced with a smaller  $k$  value, while a maximum resonator length is limited to twice that of the corresponding resonator.

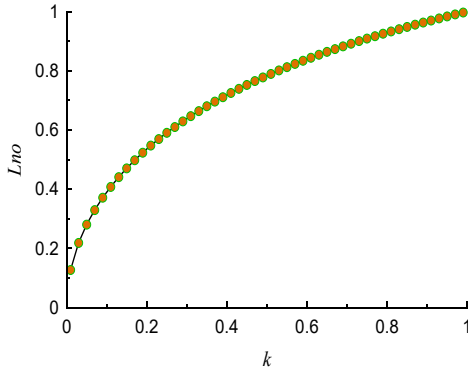


Fig. 5. Normalized length as a function of impedance ratio.

### Spurious Resonance Frequencies

Fundamental resonance frequency is represented by  $f_o$ , whilst the lowest spurious frequencies of  $\lambda_g/4$ ,  $\lambda_g/2$  and  $\lambda_g$  are represented by  $f_{SA}$ ,  $f_{SB}$  and  $f_{SC}$ , respectively. Assume  $\theta_1 = \theta_2 = \theta_o$  in the analysis. Resonator electrical lengths corresponding to spurious frequencies  $f_{SA}$ ,  $f_{SB}$  and  $f_{SC}$  are represented as  $\theta_{SA}$ ,  $\theta_{SB}$ , and  $\theta_{SC}$ , respectively. From Eqn.(3).

$$\theta_1 = \theta_2 = \theta_o \quad \text{so} \quad \tan^2\theta_o = k$$

$$\therefore \theta_o = \tan^{-1}\sqrt{k} \quad \text{for } f_{SA}$$

The resonance conditions for  $\lambda_g/2$  and  $\lambda_g$  resonators can be determined from

$$\tan\theta_o(k+1)(k - \tan^2\theta_o) = 0 \quad (13)$$

Solutions of this equation are:

$$\theta_o = \tan^{-1}\sqrt{k} \quad (14)$$

$$\theta_{SB} = \theta_{SC} = \frac{\pi}{2}$$

$$\therefore \frac{f_{SA}}{f_o} = \frac{\theta_{SA}}{\theta_o} = \frac{\pi}{\tan^{-1}\sqrt{k}} - 1 \quad (15)$$

$$\frac{f_{SB}}{f_o} = \frac{f_{SC}}{f_o} = \frac{\theta_{SB}}{\theta_o} = \frac{\pi}{2\tan^{-1}\sqrt{k}} \quad (16)$$

The fundamental and spurious frequencies should be as far as possible. Fig. 6 suggests that a  $\lambda_g/4$  resonator with a small  $k$  value should be chosen for optimal design, which simultaneously minimizes resonator length. In particular, the frequency ratio between its second and first resonant modes can be made greater than 2 for smaller magnitudes of  $k$ .

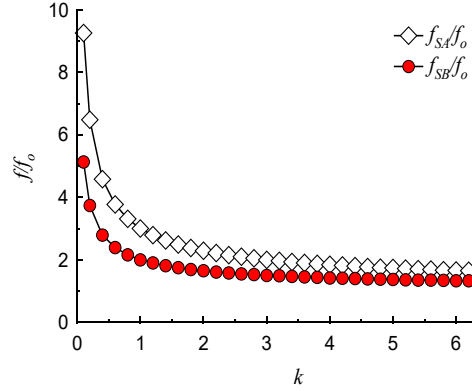


Fig. 6. Ratio of lowest spurious frequencies  $f_{SA}$  ( $\lambda_g/4$ ) and  $f_{SB}$  ( $\lambda_g/2$ ) to fundamental frequency ( $f_o$ ).

### B. Even Mode Analysis

For even-mode excitation, there is no current flow through the symmetrical plane. Thus, we can bisect the circuit with open circuits at the middle to obtain the equivalent circuit of Fig. 3(a). Ignoring the discontinuity of the folded section, the input admittance for even-mode can be approximately obtained as

$$Z_L = j \frac{Z_2}{2} \cot\theta_2 \quad (17)$$

$$Z_{ine} = jZ_1 \left\{ \frac{\frac{Z_2 + Z_1 \tan\theta_1 \tan\theta_2}{2}}{Z_1 \tan\theta_2 - \frac{Z_2}{2} \tan\theta_1} \right\} \quad (18)$$

Condition for resonance for even-mode is  $Y_{ine} = 0$ .

$$\text{so } Z_1 \tan\theta_2 - \frac{Z_2}{2} \tan\theta_1 = 0 \quad (19)$$

The above analysis reveals that the length of SLR can be reduced by increasing the impedance of the stub in relation to the resonator, i.e. reducing the impedance ratio  $k$ . Also, the spacing between the fundamental and spurious responses generated by the SLR can be increased by reducing the impedance ratio  $k$ .

## IV. WIDEBAND FILTER DESIGN AND RESULTS

Based upon the proposed SLR structure shown in Fig. 1(a), a wideband bandpass filter is synthesized with wide stopband. Feedline is via high impedance interdigital capacitor to realize

strong EM coupling to the filter structure. Stub-loaded resonators are arranged on opposite sides to each other to form a parallel resonator doublet, which has an effect to significantly widen the filter's passband. Construction of the filter was on a standard dielectric substrate Arlon CuClad217LX with thickness ( $h$ ) of 0.794 mm, dielectric constant ( $\epsilon_r$ ) of 2.17 mm, copper conductor thickness ( $t$ ) of 35  $\mu\text{m}$ , and loss-tangent ( $\tan\delta$ ) of 0.0009.

Simulation of the filter was carried out by using full wave EM simulator ADS Momentum. Magnitude of filter's parameters (in millimeter) are:  $W_a = 0.82$ ,  $W_{a1} = 0.2$ ,  $W_{a2} = 0.2$ ,  $W_{a3} = 0.2$ ,  $W_d = 1.23$ ,  $W_b = 0.2$ ,  $W_{b1} = 0.2$ ,  $W_c = 0.2$ ,  $W_{c1} = 0.2$ ,  $L_a = 6.78$ ,  $L_{a1} = 4.83$ ,  $L_{b1} = 2.55$ ,  $L_{b2} = 3.63$ ,  $L_{b3} = 11.49$ ,  $L_1 = 4.97$ ,  $L_2 = 3.3$ ,  $L_3 = 1.57$ ,  $L_4 = 1.72$ ,  $L_5 = 5.15$ ,  $L_6 = 1.09$ ,  $S_3 = 0.52$ , and  $S_4 = 0.2$ .

Effect of open-circuited stub length ( $L_a$ ) on the filter's performance is shown in Fig. 7. As the length of  $L_a$  is increased from 6.78 mm to 7.78 mm the lower transmission zero is stretched downward in frequency, and the out-of-band rejection level on left-hand side of the passband improves significantly from 15.8 dB to 32.8 dB; however, a small insertion-loss dip manifestation is created in the left corner of the passband. The length  $L_a$  has negligible effect on the upper transmission zero and rejection level. Length  $L_a$  enables the control the lower transmission zero to some extent without significantly affecting the upper transmission zero and other filter characteristics.

Fig. 8 shows as the length of the lower open-circuited stub ( $L_{a1}$ ) is reduced from 4.83 to 4.03 mm, the upper transmission zero is stretched upwards in frequency, and the out-of-band rejection level improves significantly from 14.88 dB to 28.74 dB; however, a relatively small dip is generated on the right corner of the passband. The change in length has no effect on the lower transmission zero and out-of-band rejection level. Length  $L_{a1}$  allows the manipulation of the filters upper transmission zero without affecting the other filter characteristics.

Interdigital coupled feed length ( $L_{b3}$ ) controls the out-of-band rejection level on both sides of the filter's passband, as shown in Fig. 9. Decrease in  $L_{b3}$  can cause a relatively small dip to appear at the center of the passband. The optimum value of  $L_{b3}$  is 10.28 mm.

Coupling length ( $L_5$ ) has insignificant effect on the filter's passband response. The separation gap ( $L_6$ ) has negligible effect on the filter's center frequency and the lower transmission zero. From simulation analysis it is observed that as the coupling gap is increased the out-of-band rejection improves, however this is at the expense of creating relatively large passband ripples. The optimum value of gap  $L_6$  is 0.72 mm to realize a flat passband and wide stopband with around 20 dB of rejection.

Length of the impedance section ( $L_{b2}$ ) has effect on the filter's out-of-band rejection. When the length  $L_{b2}$  is reduced the out-of-band rejection on the right-hand side of the filters' passband deteriorates significantly. With a length of 1.83 mm the rejection is around 10 dB. Although the length has no effect on the filter's center frequency however the insertion-loss increases slightly from 0.43 dB to 0.65 dB with reduction in  $L_{b2}$  from 4.83 mm to 1.83 mm.

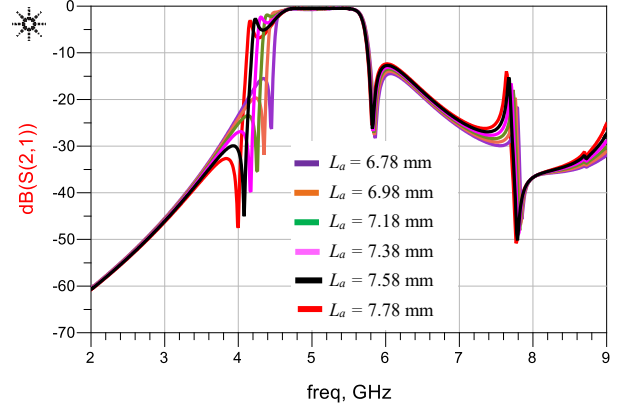


Fig. 7 Effect of stub length ( $L_a$ ) on the filter's passband response.

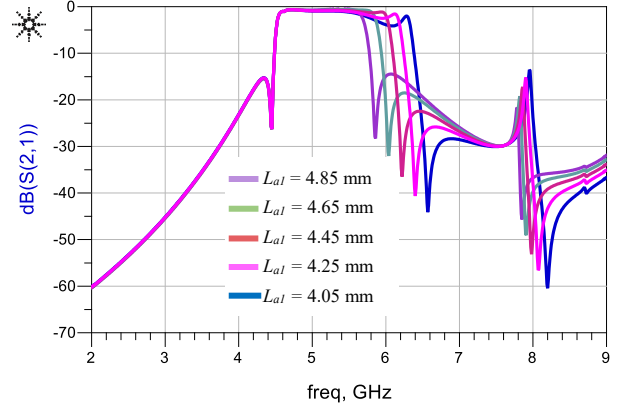


Fig. 8 Effect of stub length ( $L_{a1}$ ) on the filter's passband response.

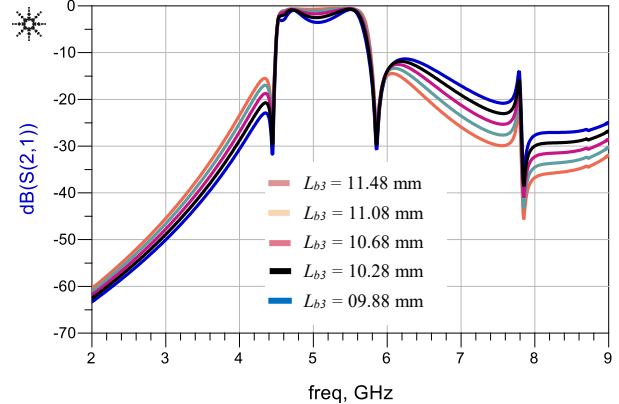


Fig. 9 Effect of interdigital feed length ( $L_{b3}$ ) on the filter's passband response.

The fabricated wideband filter is shown in Fig. 10 after extensive optimization to improve the out-of-band rejection. Frequency response of the filter close-up and full are shown in Fig. 11. The filter exhibits a very sharp passband skirt and is centered around 5.12 GHz with insertion-loss of 0.73 dB and return-loss better than 20 dB. Insertion-loss is attributed to conductor and dielectric losses. The two transmission zeros near the lower and upper cut-off frequencies that are located at 4.5 GHz and 5.74 GHz, respectively, contribute towards the filter's sharp selectivity. The 3-dB fractional bandwidth of the

filter is 24.2% and its out-of-band rejection is better than 40 dB across 2 to 4.5 GHz and 5.74 to 16 GHz. Table 1 shows comparison of the salient features of the proposed wideband bandpass filter with other microstrip quasi-elliptic filters reported. This clearly shows the proposed topology exhibits significantly better stopband rejection extending over a wide frequency range. The overall size of the filter can be reduced by folding the linear stubs.

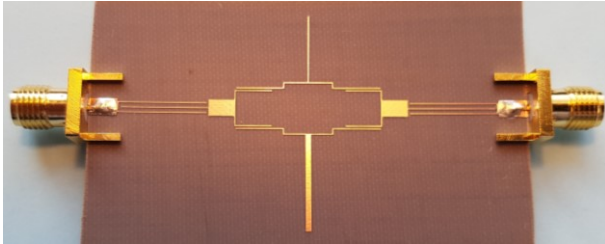


Fig. 10 Fabricated wideband filter.

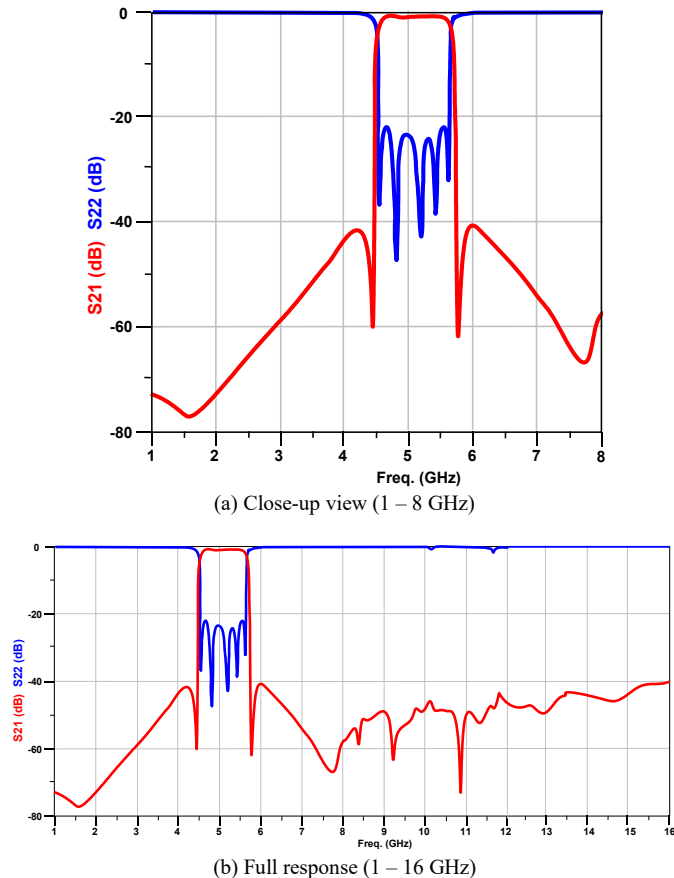


Fig. 11. Measured insertion-loss and return-loss response of the proposed wideband filter.

Table 1 – Comparison with other wideband quasi-elliptic bandpass filters. ( $f_o$  is center frequency, FBW is fractional bandwidth, and IL is passband insertion-loss)

	$f_o$ (GHz), FBW	IL (dB)	Stopband suppression	Circuit size ( $\lambda_g^2$ )
[9]	2.33, 39.8%	0.65	-15 dB (1.12 – 3.3 $f_o$ )	0.22×0.22
[10]	1.82, 24.4%	0.95	-30 dB (1.16 – 2.63 $f_o$ )	0.13×0.22
This work	5.12, 24.2%	0.73	-40 dB 1.12 – 3.125 $f_o$	1.39×0.67

## V. CONCLUSION

Realization of a novel wideband bandpass filter with high out-of-band rejection over a wide frequency range was demonstrated using planar microstrip technology. Synthesis of the via-free bandpass filter is based on stub loaded resonators. The resulting highly compact filter exhibits low insertion-loss (0.73 dB) in its passband (4.5–5.74 GHz), a sharp roll-off, steep skirt selectivity and a high stopband rejection level (>40 dB) over a large frequency range up to 16 GHz. The filter's features make it suitable for application in wideband wireless communications systems.

## REFERENCES

- [1] Y.-C. Chiou, J.-T. Kuo, and E. Cheng, "Broadband quasi-Chebyshev bandpass filters with multimode stepped-impedance resonators," *IEEE Trans. Microw. Theory Tech.*, vol. 54, no. 8, pp. 3352–3358, Aug. 2006.
- [2] A. Turkeli, A. K. Gorur, E. G. Sahin, A. Gorur, "Design of dual wideband bandpass filter using stub loaded multi-mode resonators," *Microwave & Optical Letters*, Vol. 60, Issue 10, pp. 2370-2374, Oct. 2018.
- [3] Y.-S. Lin, W.-C. Ku, C.-H. Wang, and C. H. Chen, "Wideband coplanar waveguide bandpass filters with good stopband rejection," *IEEE Microw. Wireless Compon. Lett.*, vol. 14, no. 9, pp. 422–424, Sep. 2004.
- [4] C. J. Bindu, S. Mridula, P. Mohanan, "Coplanar waveguide filter using stub resonators for ultra wide band applications," *Procedia Computer Science*, Vol. 46, pp. 1230-1237, 2015.
- [5] X. Luo, H. Qian, J.-G. Ma, and E.-P. Li, "Wideband bandpass filter with excellent selectivity using new CSRR-based resonator," *Electron. Lett.*, vol. 46, no. 20, pp. 1390–1391, Sep. 2010.
- [6] X. Luo, J.-G. Ma, K. Ma, and K. S. Yeo, "Compact UWB bandpass filter with ultra narrow notched band," *IEEE Microw. Wireless Compon. Lett.*, vol. 20, no. 3, pp. 145–147, 2010.
- [7] S. M. S. Moshiri, A. Alighanbari, A. Yahaghi, "Highly selective wideband bandpass filter using combined microstrip/coplanar waveguide structure," *Electronics Letters*, Vol. 52, Issue 13, pp. 1145-1147, June 2016.
- [8] H. Ishii, T. Kimura, N. Kobayashi, A. Saito, Z. Ma, and S. Ohshima, "Development of UWB HTS bandpass filters with microstrip stubs-loaded three-mode resonator," *IEEE Transactions on Applied Superconductivity*, vol. 23, No. 3, June 2013.
- [9] J. Xu, "Compact quasi-elliptic response wideband bandpass filter with four transmission zeros," *IEEE Microwave and Wireless Components Letters*, Vol. 25, No. 3, pp. 169-171, 2015.
- [10] J. Xu, Z.-Y. Chen, and Q.-H. Cai, "Compact quasi-elliptic wideband bandpass filter using mixed coupling lumped-element dual-resonance resonators," *Electromagnetics*, Vol. 38, No. 1, pp.70-76, 2018.